

X-ray microbeam three-dimensional topography imaging and strain analysis of basal-plane dislocations and threading edge dislocations in 4H-SiC

Silicon carbide (SiC) bipolar devices (IGBT and p-n diodes, etc.) are promising candidates for next-generation high-voltage power applications in various industries, traffic control, automobiles, and power-transmission systems. However, basal plane dislocations (BPDs) in an epilayer can cause an increase in the forward voltage drop of SiC bipolar devices, hindering their extensive commercialization. A promising method of reducing BPD density in an epilayer is to convert BPDs to threading edge dislocations (TEDs) near the epilayer/substrate (E/S) interface. To ensure perfect BPD-TED conversion, however, better understanding of the conversion mechanism is necessary [1].

X-ray microbeam three-dimensional (3D) topography has been developed for the depth-resolved crystallographic analysis of semiconductor crystals. This method enables us to investigate the behavior of dislocations near a deep E/S interface. This article describes the application of X-ray 3D topography to the study of BPD-TED conversion [2].

The sample examined is an 8°-off-cut (0001) Si-face 4H-SiC wafer with a 20- μm -thick epilayer. The setup of 3D topography measurements is shown in Fig. 1. The measurements were conducted at beamline BL24XU using an X-ray microbeam with photon energy of 15 keV. The full widths at half maximum (FWHMs) of the microbeam were typically 1.9 and 0.6 μm in the horizontal and vertical directions, respectively. The X-ray 3D topography uses a special slit with a V-shaped valley (V-slit) for microbeam X-ray diffraction. The incident X-ray penetrates the sample, generating a ribbon-shaped diffraction beam ($\mathbf{g} = 1\ 1\ \bar{2}\ 12$) that impinges on the V-slit. After passing through the V-slit, a thin X-ray beam reaches a scintillation

counter (SC) through a fully opened receiving slit (RS). We thus conducted pinpoint measurement at point Q where the incident beam intersects the extension of the beam passing through the V-slit. Scanning the sample provides a depth-resolved 3D topograph. Unlike conventional X-ray topography, dislocation images in a 3D topograph are dominated by kinematical direct images due to the extinction contrast [2].

Measurements were carried out in 3D-single-scan (3DSS) and 2D-multiscan (2DMS) modes. In the 3DSS mode, sample positions were scanned in three dimensions at a fixed ω value to obtain a 3D topograph. In the 2DMS mode, the 2D data of reflection intensities were acquired for a desired cross section at step-scanned ω values to obtain an image of effective misorientations ($\Delta\omega$ map).

Figure 2 compares the conventional back-reflection X-ray topography and the 3D topography. The conventional topography (Fig. 2(a)) shows two BPDs, one of which (BPD1) is converted to a TED (TED1), and the other (BPD2) propagates to the epilayer surface. At the same position, a 3DSS

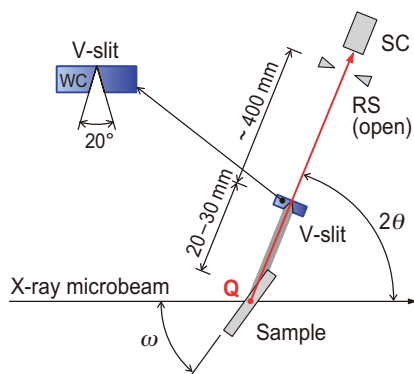


Fig. 1. X-ray diffraction geometry for 3D topography measurements. [2]

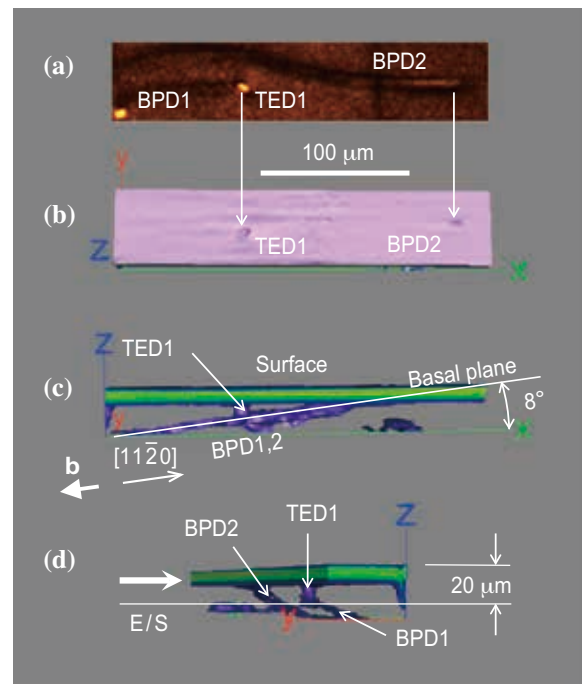


Fig. 2. X-ray 3D topography images of a TED (TED1) and two BPDs (BPD1 and BPD2) in comparison with conventional back-reflection X-ray topography. BPD1 is converted to TED1, whereas BPD2 propagates to the epilayer surface.

measurement was carried out with 2.5- μm cubic voxels within a 30- μm -deep region from the surface, providing the stereographic isosurface images shown in Figs. 2(b)-2(d). The top view (Fig. 2(b)) indicates two pits corresponding to TED1 and BPD2. The side view (Fig. 2(c)) shows that TED1 is almost perpendicular to the surface, while BPD1 and BPD2 lie on the basal plane at an angle of 8° from the surface. From the oblique camera angle (Fig. 2(d)), we can confirm that BPD2 propagates from the substrate to the epilayer, whereas BPD1 is converted to TED1 near the E/S interface at a depth of 20 μm . The horizontal high-intensity region along the surface (arrow in Fig. 2(d)) is caused by surface strain.

Figure 3 presents an expanded 3D topograph of BPD1 and TED1. This image was provided by a fine-step 3DSS measurement (1- μm cubic voxels) near the conversion point. Note here that the BPD1 image narrows just before the conversion as indicated by the thick arrow. Similar narrowing was also observed in other BPD-TED conversion cases. However, such narrowing did not occur in non-conversion cases such as BPD2. It is known that BPDs in a substrate are dissociated into pairs of partial dislocations separated by a stacking fault, and the two partial dislocations are constricted before converting to TEDs [3]. We consider that the narrowing of BPD1 is related to the constriction of the partial dislocations before the conversion.

Strain analysis was conducted on TED1 for cross sections perpendicular and parallel to the sample surface (C_{ZY} and C_{XY} , respectively, in Fig. 3). The 2DMS measurements were carried out with 1- μm square pixels at relative ω values ranging over ± 84 μrad with an interval of 7 μrad . The $\Delta\omega$ map for C_{ZY} is shown in Fig. 4(a), where the surface corresponds to the level of $z = 0$. In this figure, BPD1 appears from behind and converts to TED1 at a depth of about 20 μm below the surface. The positive $\Delta\omega$ along the surface (dashed ellipse) indicates compressive strains, which are responsible for the superficial high-intensity region shown in Fig. 2. Figure 4(b) shows the $\Delta\omega$ map for C_{XY} . The TED is confirmed by analysis of the conventional synchrotron back-reflection X-ray

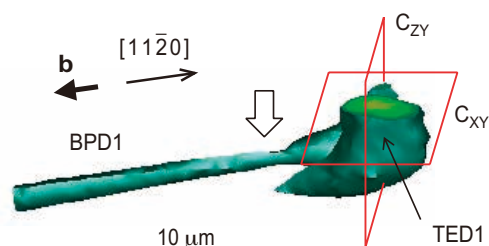


Fig. 3. Fine 3D topography image near BPD-TED conversion point.

topography to have a Burgers vector \mathbf{b} pointing in the opposite direction to the step-flow $[1\ 1\ \bar{2}\ 0]$ direction and to create an extra half-plane towards the left side [4]. Strain analysis indicates compressive and tensile strains on the left and right sides, respectively, which correlate to the direction of the extra half-plane. Strain on the order of $\pm 10^{-5}$ around the TED is revealed from the value of $\Delta\omega$ (± 10 μrad). Figure 4(c) shows the line profile ($\Delta\omega$) and its difference curve ($-\delta\Delta\omega$) along the dashed line L in Fig. 4(a). The peak width (FWHM) of $-\delta\Delta\omega$ indicates that the imaging spatial resolution is 1-2 μm .

We now have a new methodology of imaging and strain analysis using X-ray diffraction. X-ray 3D topography is useful for not only research on SiC-related materials, but also the strain analysis of dislocations and microstructures in various semiconductor crystals.

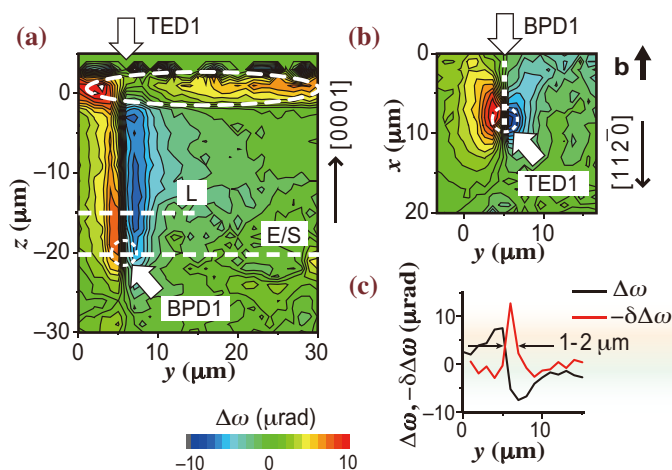


Fig. 4. Strain analysis of a TED. (a) $\Delta\omega$ map for the cross section C_{ZY} in Fig. 3. (b) $\Delta\omega$ map for the cross section C_{XY} in Fig. 3. (c) Line profile ($\Delta\omega$) and its difference curve ($-\delta\Delta\omega$) along line L in (a). [2]

Ryohei Tanuma

Materials Science Research Laboratory,
Central Research Institute of Electric Power Industry (CRIEPI)

Email: tanuma@criepi.denken.or.jp

References

- [1] H. Tsuchida *et al.*: Phys. Status Solidi B **246** (2009) 1553.
- [2] R. Tanuma, D. Mori, I. Kamata and H. Tsuchida: Appl. Phys. Express **5** (2012) 061301.
- [3] S. Chung *et al.*: J. Appl. Phys. **109** (2011) 094906.
- [4] I. Kamata *et al.*: J. Cryst. Growth **311** (2009) 1416.